

## ANOMALOUS REDSHIFTS OF QUASI-STELLAR OBJECTS

J. V. NARLIKAR

Tata Institute of Fundamental Research, Bombay 400 005

AND

P. K. DAS

Indian Institute of Astrophysics, Bangalore 560 034

Received 1979 December 27; accepted 1980 March 5

## ABSTRACT

This paper is based on the assumption that the observational evidence to date does point to the possibility that high-redshift quasars are physically associated with low-redshift galaxies. It is first argued that the excess (or *anomalous*) redshifts of the quasars in such associations are unlikely to be either of Doppler or of gravitational origin. A new source for this excess redshift was suggested by Narlikar on the basis of the Hoyle-Narlikar theory of gravitation which is based on Mach's principle. This idea is applied to the hypothesis that quasars may have been ejected from galactic nuclei. The dynamics of such an ejection and its observable consequences are discussed. In particular, it is shown that quasar alignments and redshift bunching which have been observed recently can be understood within the framework of this theory. Further tests of this hypothesis are discussed.

*Subject headings:* cosmology — gravitation — quasars

## I. INTRODUCTION

In spite of the many observational advances in extragalactic astronomy, the interpretation of the nature of redshifts of quasars continues to be a subject of controversy. We do not wish to enter here into the various issues of this controversy, but will concentrate on only one of the observational criteria used in this connection. This test is based on the search for apparent associations between quasars and galaxies.

The underlying assumption of this test is that the redshift of a typical galaxy is of cosmological origin, i.e., arising from the expansion of the universe. If a definite physical association can be established between a quasar and a galaxy, then it can be concluded that the two are in the same part of the universe and hence should have the same cosmological redshift. If  $z_G$  is the redshift of the galaxy and  $z_Q$  the redshift of the quasar, then the result  $z_Q \approx z_G$  establishes that the quasar redshift is also of cosmological origin. On the other hand, the result  $z_Q \neq z_G$  indicates the contrary, i.e., that the quasar may have an "anomalous" noncosmological component of redshift.

This test has been used by both sides in the redshift controversy. A detailed discussion of the observational situation in this respect has been given by Stockton (1978), Burbidge (1979), and Arp (1977), and we can do no better than refer the reader to the different points of view expressed therein.

However, we feel that the interpretation of anomalous redshifts as merely a series of chance coincidences has become more and more difficult to sustain in view of the recent data on alignments and redshift bunching. For example, Arp, Sulentic, and di Tullio (1979) have reported six quasars in the neighborhood of the galaxy NGC 3384 with alignments of quasars of similar redshifts across the galaxy. Arp (1980*a*) has further found striking alignments of quasars in the neighborhood of NGC 2639. In such alignments there is also a bunching of redshifts of quasars. For example, in NGC 2639, quasars with redshifts 1.52 and 1.53 are found on the opposite sides of the galaxy. Similar quasar pairs with nearly equal redshifts near  $z_Q = 0.30$  and 2 are found in this configuration. Analysis of quasars in the CTIO Curtis Schmidt survey in the  $5^\circ$  zone  $-37.5 > \delta > -42.5$  and R.A. from  $20^h$  to  $6^h$  by Arp (1980*b*) shows a bunching of redshifts for quasars with  $z_Q > 2.5$ , and there is evidence in several cases of quasars of almost identically equal redshift value pairing across an associated galaxy.

But perhaps the most remarkable configuration is of a pair of triplets of quasars, discovered by Arp and Hazard (1979) by the objective prism method. In the area designated by Hazard as 1130 + 106, these authors have reported three quasars *A*, *B*, *C* ( $z_A = 0.54$ ,  $z_B = 2.12$ ,  $z_C = 1.61$ ) in a straight line together with another set of three quasars *X*, *Y*, *Z* ( $z_X = 2.15$ ,  $z_Y = 0.51$ , and  $z_Z = 1.72$ ) in a straight line. It would be extremely difficult to explain these alignments on a chance basis. The above configuration has another remarkable feature which we will refer to in § V.

In this paper we take the view that the effects discussed above are real and need to be explained. The explanation must first tell us why, if a quasar and a galaxy exit close to each other, we have  $z_Q > z_G$ . In addition we need an understanding of the effect which leads to the dependence  $\theta \propto z_G^{-1}$  observed for such pairs. Finally the

theory should throw some light on the alignments and redshift bunching which have been briefly described above. Clearly, cosmological redshift alone cannot account for these phenomena, since this redshift depends only on the distance of the observer from the source. Instead we have to look for an explanation involving some intrinsic property of these quasars and galaxies.

## II. NONCOSMOLOGICAL REDSHIFTS: CONVENTIONAL ALTERNATIVES

There are two conventional alternatives to account for the anomalous redshift of a quasar. One is the Doppler shift; the other is the gravitational redshift. Let us consider these alternatives in the light of the available data.

If, as Arp has argued on several occasions, the quasars have been ejected from galaxies then for sufficiently high ejection velocities ( $v \approx c$ ), large Doppler shifts can arise. The Doppler redshift is given by

$$1 + z = \left( \frac{1 + v/c}{1 - v/c} \right)^{1/2}. \quad (1)$$

A redshift  $z = 2$  corresponds to  $v = 0.8c$ . In the purely local theory of quasars first put forward by Terrell (1964) the quasars were assumed to have been ejected from the nucleus of our Galaxy. Velocities of such high magnitude would, however, pose severe energy problems as well as stability problems for our Galaxy. For this reason Hoyle and Burbidge (1966) proposed the exploding nuclei of galaxies like NGC 5128 as likely sites for the ejection of quasars.

The alignments and similarities of redshifts of quasars around galaxies in the data discussed in § I no doubt suggest the Doppler effect as an attractive alternative. There are similar models based on observed alignments, for radio sources where a central nucleus is supposed to have ejected two blobs of plasma in opposite directions. The quasars may well have been ejected in a similar fashion from the associated galaxy.

However, there is a basic difficulty associated with this interpretation for the present case, viz., the total lack of blueshifted quasars. Since the galaxy redshift is usually small, the bulk of the quasar redshift must be due to the large ejection velocities. If an exploding source is ejecting quasars in all directions, some of these must come toward us instead of receding from us and hence must show large blueshifts. In fact, calculations done in the case of isotropic ejection in a flux-limited sample show that the blueshifted quasars must predominate in large numbers (Burbidge and Burbidge 1967). Still, not a single blueshifted quasar has yet been observed. This complete absence of blueshifted quasars, especially in the quasar-galaxy systems with alignments, makes the Doppler effect alternative of doubtful value, if not totally invalid.

The second alternative, that of a gravitational redshift, has its own difficulties. First, it has been shown by Bondi (1964) that the surface redshift of any object in equilibrium under realistic equations of state ( $p \lesssim \frac{1}{3}\rho$  in the core and  $dp \lesssim d\rho$  in an adiabatically stable envelope) cannot exceed 0.62. Thus at best only a small fraction of the high redshift in a quasar can arise from a gravitation potential well at the surface of the quasar.

Later Hoyle and Fowler (1967) proposed a model in which large redshifts could be obtained from the center of the quasar. For this the quasar has to have an optically thin envelope which nevertheless has enough matter to provide a deep enough potential well at the center. Although in a Schwarzschild interior solution the central redshifts can be arbitrarily large, Bondi's energy condition is violated. Das and Narlikar (1975) showed that it is possible to satisfy Bondi-type equations of state and still get central redshifts as high as  $z_0 \gtrsim 2$ . The spectroscopic characteristics, stability under small oscillations, the positivity of velocity distribution functions, and other physical and astrophysical requirements place further restrictions on these models (Das 1976).

Although such considerations do not yet rule out quasar models of gravitational redshifts as high as 2, they make quasars rather esoteric objects. Even granted that the quasars have peculiar characteristics, it becomes difficult to see in this theory why there should be associations between quasars and galaxies. Thus while these models could still be viable ones for isolated quasars, they cannot be considered satisfactory for quasars found in associations with galaxies.

In view of these difficulties with the conventional models, the data on anomalous redshifts force one to look for other alternatives even though they involve unconventional ideas. We shall be concerned with one such approach in the rest of this paper.

## III. REDSHIFT FROM VARIABLE PARTICLE MASSES

### a) A Machian Theory of Gravity

In 1964, Hoyle and Narlikar proposed a theory of gravity which had its origin in Mach's principle. According to this theory every particle in the universe derives its inertia from the rest of the particles in the universe. Just as the Fokker action describes action-at-a-distance electrodynamics in a relativistically invariant manner, inertia is described here as an action-at-a-distance phenomenon in a generally covariant way. The Hoyle-Narlikar (HN) theory is not only coordinate invariant in a Riemannian manifold, like general relativity, it is also *conformally* invariant. The details of the HN theory and its connection with electrodynamics are described elsewhere in detail (Hoyle and Narlikar 1974). Here we consider those aspects of it which are relevant to the present discussion.

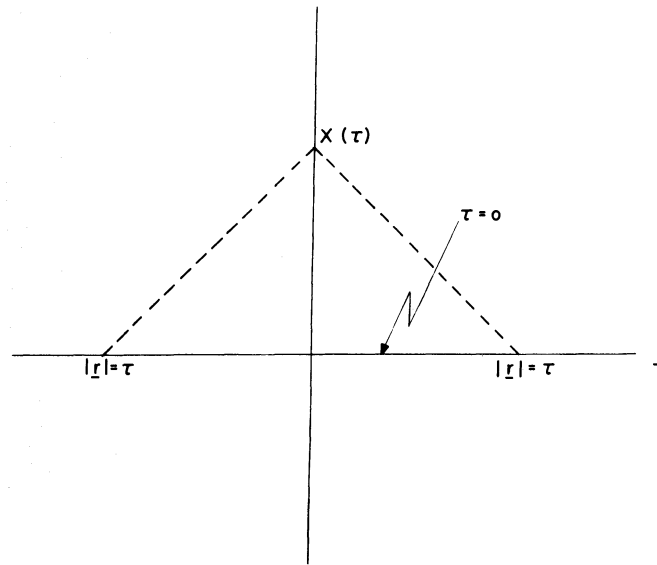


FIG. 1.—The Machian contribution to the inertia at  $X$  comes from all the particles whose world lines intersect the  $\tau = 0$  hypersurface inside the past light cone from  $X$ .

Consider the Einstein–de Sitter cosmology, which is a solution of Einstein’s field equations for a homogeneous, isotropic distribution of dust. The line element of this spacetime manifold  $\mathfrak{M}_E$  is given by

$$ds^2 = dt^2 - (3t/2)^{4/3} [dr^2 + r^2(d\theta^2 + \sin^2 \theta d\phi^2)]. \quad (2)$$

We have taken the Hubble constant at the present epoch ( $H_0 = 50 \text{ km s}^{-1} \text{ Mpc}^{-1}$ ) to be unity. The velocity of light is also taken to be unity. This means that the times are measured in units of  $\sim 6 \times 10^{17} \text{ s}$  and lengths in units of  $\sim 1.8 \times 10^{28} \text{ cm}$ . If, in addition, we also take the gravitational constant  $G$  to be unity, the mass unit is fixed as  $\sim 2.5 \times 10^{56} \text{ g}$ . Thus a galaxy of mass  $10^{11} M_\odot$  would have a mass of  $8 \times 10^{-13}$  in these units.

In general relativity, particle masses are constant. In the HN theory, on the other hand, particle masses can vary with space and time. If  $m(X)$  denotes the mass of a typical particle at a point  $X$  in spacetime and  $g_{ik}(X)$  is the metric tensor at  $X$  in any given solution of the gravitational equations of the HN theory, then for any  $\Omega(X)$  which is finite ( $0 < \Omega < \infty$ ) and twice differentiable,  $\Omega^{-1}m(X)$ ,  $\Omega^2 g_{ik}(X)$  are also solutions for the mass function and the metric tensor, respectively. In the simplest approximation  $m(X) = \text{constant}$  reduces the HN theory to general relativity.

It follows, therefore, that from (2) we can construct another solution of the HN field equations by a conformal transformation

$$\Omega = (3t/2)^{-2/3}. \quad (3)$$

If we make a coordinate transformation

$$\tau = (12t)^{1/3}, \quad (4)$$

we can make the “new” solution manifestly that of Minkowski spacetime  $\mathfrak{M}$ :

$$ds^2 = d\tau^2 - dr^2 - r^2(d\theta^2 + \sin^2 \theta d\phi^2). \quad (5)$$

The particle mass function is no longer constant but has the epoch dependence given by

$$m(\tau) = \mu\tau^2, \quad \mu = \text{constant}. \quad (6)$$

The Machian nature of the HN theory now becomes clear. In Figure 1 we have the spacetime diagram for (5) with  $X$  a point with epoch  $\tau > 0$ . From  $X$  we draw the past light cone which intersects  $\tau = 0$  in a sphere of radius  $\tau$ . If a typical particle within the sphere  $\Sigma$  contributes an inertia  $\lambda r^{-1}$ , where  $\lambda$  is a coupling constant, the total contribution from all particles inside the sphere is given by

$$\int_0^\tau \frac{\lambda}{r} \times 4\pi r^2 n dr = 2\pi n \lambda \tau^2, \quad (7)$$

where  $n$  = number density of particles. Thus, the constant  $\mu$ , which measures the magnitude of the inertia at  $X$ , is related to the number of particles inside the past sphere of influence  $\Sigma$  of  $X$ .

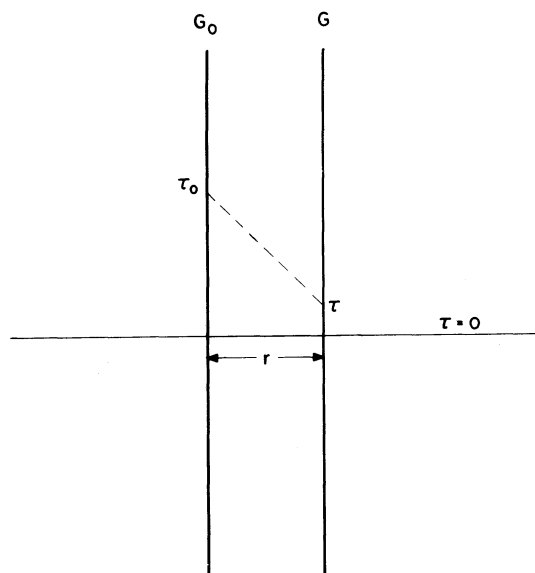


FIG. 2.—The world lines of two galaxies  $G$  and  $G_0$  in the Minkowski spacetime manifold with epoch dependent particle masses. The masses vanish on the spacelike hypersurface  $\tau = 0$ . A ray of light leaving  $G$  at epoch  $\tau$  reaches  $G_0$  at the epoch  $\tau_0 = \tau + r$ , where  $r$  is the distance of  $G$  from  $G_0$ .

The cosmological redshift can be reinterpreted in the new spacetime in the following way. Let  $G_0$  be the world line of our Galaxy (see Fig. 2) and  $\tau_0$  the present epoch of observation. A galaxy  $G$  located at a distance  $r$  is seen by us as it was at the epoch  $\tau = \tau_0 - r$ . The masses of elementary particles in  $G$ , as seen by us, were  $\mu(\tau_0 - r)^2$ , whereas in our own Galaxy at the present epoch they are  $\mu\tau_0^2$ . In flat spacetime there is no change in the frequency and hence no redshift arising from the passage of light through spacetime. However, the frequency does vary in proportion to the mass of the emitting particle in the atom. So the wavelengths of light from  $G$  look longer, compared to those in  $G_0$ , because they have always been that way since their origin from lighter particles. The redshift is therefore simply given by the fractional increase of particle mass from the epoch  $(\tau_0 - r)$  to the present epoch:

$$z_G = \frac{\tau_0^2}{(\tau_0 - r)^2} - 1. \quad (8)$$

Transformation back to the  $(r, t)$  coordinates reproduces the familiar redshift formula of the Einstein–de Sitter cosmology.

Hoyle (1975) has discussed the advantages of this way of looking at the standard Friedman cosmology. In particular, he has pointed out that the Minkowski spacetime  $\mathfrak{M}$  is easily extendable to  $\tau < 0$ , and one can relate the radiation generated in the “past half” of the universe to the origin of the cosmic microwave background. The small particle masses close to the  $\tau = 0$  epoch act as efficient thermalizers of this radiation. Such an approach is therefore able to account for the photon-to-baryon number ratio in the universe.

The usual spacetime singularity at  $t = 0$  in the Einstein–de Sitter cosmology is transformed away in  $\mathfrak{M}$ , although it is replaced by a zero mass hypersurface. Kembhavi (1978) has shown this to be a general feature of singularities in relativistic cosmology. If we start with a nonsingular solution in the HN cosmology, we can generate from it a solution of relativistic cosmology, by a conformal transformation. However, the transformation is invalid at a zero mass hypersurface where the condition  $0 < \Omega < \infty$  is violated. This violation manifests itself as a spacetime singularity.

#### b) Anomalous Redshifts

Although the interpretation of cosmic microwave background and the spacetime singularity are simplified in the above approach, so far as the redshift is concerned we have not gained anything new. The formula (8) is the usual expression for the cosmological redshift in a different form. To get something different—e.g., anomalous redshifts—we have to introduce small-scale inhomogeneities into the above cosmological picture. A way to do this was discussed by Narlikar (1977) along the lines summarized below.

In the cosmological solution described above, all particles have zero mass at the same epoch  $\tau = 0$ . This is because the positive and negative inertial contributions from the two halves of the homogeneous universe exactly cancel at  $\tau = 0$  for every particle.

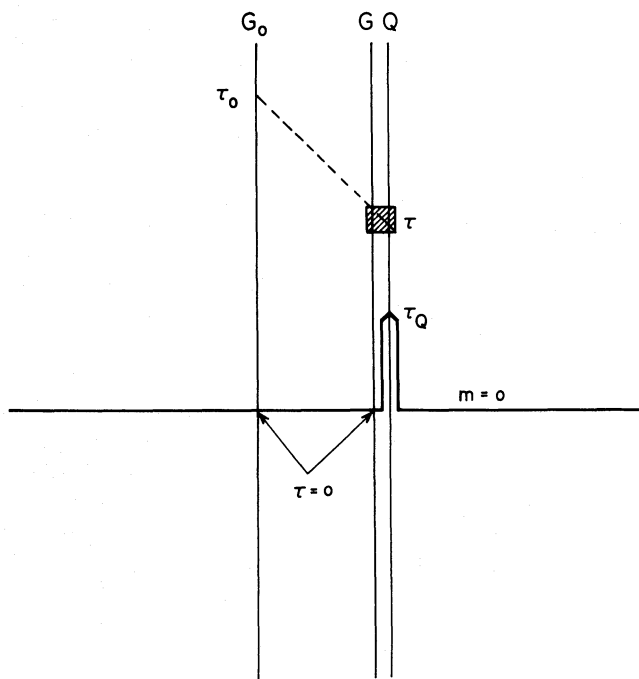


FIG. 3.—A kink in the zero mass hypersurface. The world line of the quasar  $Q$  crosses this kink with the result that particles in  $Q$  have masses smaller than those of the particles in a neighboring galaxy  $G$  whose world line does not cross the kink.

Suppose instead that there are local inhomogeneities which lead to kinks in the zero mass hypersurface. One such kink is shown in Figure 3. It was pointed out by Narlikar (1977) that the local distortions in the zero mass surface can be looked upon as an implosion followed by an explosion. That is, prior to the zero mass surface a local inhomogeneity of matter collapses in much the same way that the extended Friedmann model described in § IIIa collapses in the region  $\tau < 0$ . And, like the cosmological model, this local collapse is followed by a local explosion. Since the collapse builds up local regions of high density, we expect to see the corresponding explosions come out of such dense regions. Galactic nuclei are therefore ideal sites for observing these local explosions. We accordingly suggest that quasars may be born out of explosions in galactic nuclei.

From the detailed discussion given by Hoyle (1975) about the state of matter as it approaches the zero mass surface, it seems likely that the matter which emerges from the explosion would be lumpy rather than homogeneous. Thus the quasars emerge from the explosion as discrete compact objects. We emphasize, however, that we have no detailed theory about the structure of quasars. The arguments that follow simply make use of the hypothesis that quasars correspond to kinks in the zero mass surface.

With this picture in mind we look at the kink in Figure 3. Here an object  $Q$  has particles whose zero mass occurs at a later epoch:  $\tau_Q > 0$ . Calculation of the mass of a typical particle in  $Q$  at the epoch  $\tau > \tau_Q$  shows (see Narlikar 1977 for details) that

$$m_Q = \mu(\tau - \tau_Q)^2. \quad (9)$$

Such kinks which can be identified with the origins of quasars are few and far between, so the majority of matter has  $m = 0$  at  $\tau = 0$ . This "normal" matter determines the dynamics of the universe as a whole. The cosmological solution is therefore unaltered.

If a galaxy  $G$  of normal particles (i.e., particles with zero mass epoch at  $\tau = 0$ ) happens to be close to  $Q$ , the particle masses in  $G$  will be

$$m_G = \mu\tau^2. \quad (10)$$

Suppose  $G$  and  $Q$  are near neighbors and let light waves from them leave at the epoch  $\tau$  and reach an observer in  $G_0$  at the epoch  $\tau_0$ . This observer will compare the wavelengths of light from  $G$  and  $Q$  to the wavelengths he would expect from particle masses  $m_{G_0}$  in his own neighborhood. Assuming that  $G_0$  is made of normal particles,

$$m_{G_0} = \mu\tau_0^2. \quad (11)$$



The observer in  $G_0$  will therefore find the redshifts  $z_G$  and  $z_Q$  (of  $G$  and  $Q$ ) to be different:

$$z_G = \tau_0^2/\tau^2 - 1, \quad z_Q = \tau_0^2/(\tau - \tau_Q)^2 - 1. \quad (12)$$

Also  $\tau_Q > 0$  implies  $z_Q > z_G$ .

If we now interpret this picture from the conformal frame in which particle masses in  $G_0, G, \dots$  are constant, we see that the epoch  $\tau_Q$  corresponds to a mini-explosion (just  $\tau = 0$  corresponds to the big bang) which gives rise to  $Q$ . If  $G$  and  $Q$  are genuinely associated, then we may consider  $Q$  as being born in an explosion in the nucleus of  $G$ . In this way we arrive at a slightly different theoretical interpretation of Arp's picture that quasars are born in galactic explosions.

The difference arises in the sense that when the quasar is ejected in an explosion, the masses of particles in it grow from zero. If the mass of an electron in  $G$  in the constant mass conformal frame is  $m_0$ , the mass of the electron in the newly born quasar will grow according to the formula

$$m = m_0[1 - (t_Q/t)^{1/3}]^2. \quad (13)$$

Thus the process of ejection does not have to involve a lot of energy in the initial stages, as the particle masses are very small. We also see qualitatively why  $z_Q > z_G$  and why the opposite cases with  $z_Q < z_G$  are not permitted. The latter cases correspond to  $\tau_Q < 0$ , i.e., quasars born prior to the big bang. Such quasars cannot survive the high temperature and high density era close to the big bang. Hence only cases with  $\tau_Q > 0$  and  $z_Q > z_G$  are seen.

In the following two sections we study the details of the dynamics of ejection since these will tell us what observations can be made to test this theory. As the motion of an object with time-dependent mass presents certain novel features, we will first discuss it in some detail.

#### IV. MOTION OF A QUASAR FIRED FROM A GALAXY

In § III we considered the universe in two different conformal frames. In the Minkowski frame, the majority of matter has  $m = 0$  on  $\tau = 0$ , while a few isolated cases (which are identified with quasars) reflect perturbations of the zero mass surface with  $m = 0$  occurring at various epochs  $\tau > 0$ . When we go over to the standard Einstein-de Sitter cosmology, the masses of particles of normal matter become constant but the masses of matter in quasars are still time dependent. In this conformal frame, which can be called the Einstein conformal frame, the equations of HN cosmology for normal matter become those of general relativity. Since the gravitational effect of the more recently created matter is negligible, we can use Einstein's field equations to determine the spacetime in the neighborhood of a galaxy. In calculating the trajectories of quasars, however, we have to keep in mind the fact that their masses vary with time even in the Einstein conformal frame.

We first discuss the line element in the neighborhood of a galaxy and then consider the equations of motion. For this purpose we will assume that most of the mass of the galaxy is concentrated in a small nuclear region and is spherically symmetric.

##### a) Inhomogeneous Spherically Symmetric Spacetime

Consider the following coordinate transformation of (2):

$$R = r\left(\frac{3t}{2}\right)^{2/3}, \quad T = \frac{2}{3}\left[\frac{1}{2}r^2 + \left(\frac{3t}{2}\right)^{2/3}\right]^{3/2}. \quad (14)$$

In terms of the  $R, T$  coordinates the line element (2) becomes

$$ds^2 = e^\nu dT^2 - e^\lambda dR^2 - R^2(d\theta^2 + \sin^2\theta d\phi^2), \quad (15)$$

where

$$e^\nu = \frac{3t}{2}(YX^2)^{-1}, \quad e^\lambda = \left(\frac{3t}{2}\right)^{1/3} Y^{-1},$$

$$X = \left[\frac{1}{2}r^2 + \left(\frac{3t}{2}\right)^{2/3}\right]^{1/2} \equiv \left(\frac{3T}{2}\right)^{1/3}, \quad Y = \left(\frac{3t}{2}\right)^{1/3} - r^2\left(\frac{3t}{2}\right)^{-1/3}. \quad (16)$$

For  $r^2 \ll t^{2/3}$ , we get  $T \approx t$  and

$$\partial t/\partial T \approx 1, \quad \partial t/\partial R \approx -2R/3T. \quad (17)$$

Under these approximations

$$e^\nu \approx 1 + \frac{1}{2}r^2(3t/2)^{-2/3}, \quad e^\lambda \approx 1 + r^2(3t/2)^{-2/3}. \quad (18)$$

Note that  $r^2 \ll t^{2/3}$  also corresponds to  $R \ll T$  and we can rewrite (18) in the form

$$e^{\nu} \approx 1 + \frac{2}{9} \left( \frac{R}{T} \right)^2 + O \left( \frac{R}{T} \right)^4, \quad e^{\lambda} = 1 + \frac{4}{9} \left( \frac{R}{T} \right)^2 + O \left( \frac{R}{T} \right)^4. \quad (19)$$

The local region near  $R = 0$  over which the metric can be considered a reasonable approximation to flat metric is determined by the condition  $R \ll T$ . If we had a spherical galaxy of mass  $M$  centered on  $R = 0$ , the local spacetime would be modified to the Schwarzschild spacetime:

$$ds^2 = \left( 1 - \frac{2M}{R} \right) dT^2 - \left( 1 - \frac{2M}{R} \right)^{-1} dR^2 - R^2 (d\theta^2 + \sin^2 \theta d\phi^2). \quad (20)$$

If we are sufficiently far from the galaxy, its gravitational pull will be negligible and the spacetime metric will be adequately given by (19), whereas very close to the galaxy the effect of universal expansion will be negligible and (20) is a good approximation. The two terms  $2M/R$  and  $2R^2/9T^2$  are comparable at the radial coordinate given by

$$R = R_c \equiv (9MT^2)^{1/3}. \quad (21)$$

For a galaxy of mass  $10^{11} M_{\odot}$ ,  $M = 8 \times 10^{-13}$ . At the present epoch  $T \sim 1$ . Hence  $R_c \sim 2 \times 10^{-4}$ . Thus for  $R \ll R_c$  the local gravitational effect of the galaxy will be important whereas for  $R \gg R_c$  the effect of the expanding universe will be important.

For the discussion of the quasar-galaxy associations it turns out that  $R \sim R_c$  and hence neither of the two effects can be neglected. An exact approach to the problem would require the solution of Einstein's equations for a central spherical mass  $M$  with the cosmological boundary conditions. Since, however,  $2M/R_c = 2R_c^2/9T^2 \sim 10^{-8}$ , we can justifiably use a linearized approximation in the present problem and write

$$e^{\nu} \approx 1 - \frac{2M}{R} + \frac{2}{9} \left( \frac{R}{T} \right)^2 + \dots, \quad e^{\lambda} \approx 1 + \frac{2M}{R} + \frac{4}{9} \left( \frac{R}{T} \right)^2 + \dots \quad (22)$$

#### b) Derivation of the Equations of Motion of the Quasar

We will consider a quasar radially fired from the galaxy. The equations of motion of a particle in the HN cosmology (Hoyle and Narlikar 1974) are given by

$$\frac{d}{ds} \left( m \frac{dx^i}{ds} \right) + m \Gamma_{kl}^i \frac{dx^k}{ds} \frac{dx^l}{ds} = g^{ik} m_{,k}. \quad (23)$$

The mass of a quasar depends only on the epoch  $t$ , as seen in §IIIb. However,  $t$  is a function of  $T$  and  $R$ . Hence we have to take into account terms like  $\partial m / \partial T$  and  $\partial m / \partial R$ .

The  $T$ -component of (23) gives, after some manipulation,

$$\frac{d}{dT} (m e^{\nu} D^{-1}) + \frac{1}{2} m D^{-1} \left[ \dot{R}^2 \frac{\partial}{\partial T} (e^{\lambda}) - \frac{\partial}{\partial T} (e^{\nu}) \right] = D \frac{\partial m}{\partial T}, \quad (24)$$

where  $\dot{R} = dR/dT$  and

$$D = (e^{\nu} - e^{\lambda} \dot{R}^2)^{1/2} = \frac{ds}{dT}. \quad (25)$$

The operator  $d/dT$  denotes rate of change along the trajectory; i.e., it is the "total" time derivative. Hence,

$$\frac{dm}{dT} = \frac{\partial m}{\partial T} + \frac{\partial m}{\partial R} \dot{R} = \frac{dm}{dt} \left( \frac{\partial t}{\partial T} + \frac{\partial t}{\partial R} \dot{R} \right). \quad (26)$$

Then (24) may be rewritten as

$$\frac{d}{dT} e^{\nu} + \frac{d}{dt} (\ln m) \left[ (e^{\nu} - D^2) \frac{\partial t}{\partial T} + e^{\nu} \frac{\partial t}{\partial R} \dot{R} \right] + \frac{1}{2} \left[ \dot{R}^2 \frac{\partial}{\partial T} (e^{\lambda}) - \frac{\partial}{\partial T} (e^{\nu}) \right] = e^{\nu} \frac{d}{dT} (\ln D). \quad (27)$$

We simplify (27) with the aid of (22) and (25) and then use the transformation

$$\dot{R} = x e^{(\nu - \lambda)/2}. \quad (28)$$

Finally, with the substitution of (17) and with  $e^y \approx e^{-\lambda} = (1 - 2M/R)$ , we obtain

$$\dot{x} = -(1 - x^2) \left\{ \frac{M}{R^2} + \frac{d}{dt} (\ln m) \left[ x - \frac{2R}{3T} \left( 1 - \frac{2M}{R} \right) \right] \right\} - \frac{2R}{9T^2} \left[ 1 - x^2 - \frac{2R}{T} \frac{x(1 - x^2)}{1 - 2M/R} \right]. \quad (29)$$

The three terms on the right-hand side respectively represent the effects of the gravitating central mass, the variability of the quasar mass, and the expansion of the universe.

Since in the present approximation  $t \approx T$ , we can express  $d(\ln m)/dt$  as a function only of  $T$ . Let  $t_Q \approx T_Q$  denote the epoch when the quasar was born. We then have from (4) and (9)

$$\frac{d}{dt} (\ln m) = \frac{2}{3} \frac{T_Q^{1/3}}{T(T^{1/3} - T_Q^{1/3})}. \quad (30)$$

The radial equation of motion is therefore given by (29), together with the defining relations (28) and (30). Note that within the present approximation,  $x$  is very close to  $\dot{R}$ .

### c) Solution of the Equations of Motion

The equations (28)–(30) cannot be solved analytically in terms of known functions. A numerical approach is therefore necessary. Here the main difficulty arises from the singularities at  $R = 0$ ,  $T = T_Q$ . The difficulty is, however, not of a fundamental nature. The singularity at  $R = 0$  can be circumvented by starting the motion at  $R = R_1 > 0$ . The essential feature of the problem is not lost if we assume that the mass  $M$  is concentrated within  $R \lesssim R_1$ , where  $R_1 \sim 1/10$  of the radius of the galaxy. (If need be, we can later consider the more exact problem wherein the density distribution of matter in the galaxy is taken into account.)

The equations can be integrated analytically in the very early stages, close to the time singularity  $T = T_Q$ . The dominant term in this early stage is that containing  $d(\ln m)/dt$ , and the equation of motion approximates to

$$\frac{dx}{dT} \approx -(1 - x^2) \frac{2}{3} \frac{x}{T} \frac{T_Q^{1/3}}{(T^{1/3} - T_Q^{1/3})}. \quad (31)$$

This integrates to

$$x \approx \left\{ 1 + A \left( \frac{T^{1/3} - T_Q^{1/3}}{T^{1/3}} \right)^4 \right\}^{-1/2}, \quad (32)$$

giving

$$\dot{R} \approx \left( 1 - \frac{2M}{R} \right) \left\{ 1 + A \left( \frac{T^{1/3} - T_Q^{1/3}}{T^{1/3}} \right)^4 \right\}^{-1/2}. \quad (33)$$

We see that at  $T = T_Q$ ,  $\dot{R} \approx (1 - 2M/R)$ ; i.e., the quasar is fired along a null trajectory. However, its trajectory becomes timelike at  $T > T_Q$ . Writing  $T = T_Q + \eta$ , with  $\eta \ll T_Q$ , we get

$$\dot{R} \approx [1 + (\eta/\eta_0)^4]^{-1/2}, \quad \eta_0 = 3T_Q A^{-1/4}. \quad (34)$$

The relativistic time dilatation factor  $\gamma$  is given by

$$\gamma \approx (1 - \dot{R}^2)^{-1/2} \approx (\eta_0/\eta)^2 [1 + (\eta/\eta_0)^4]^{1/2}. \quad (35)$$

The parameter  $\eta_0$  characterizes the initial motion. It denotes the time span over which the motion is relativistic. For  $\eta = \eta_0$ , we have  $\gamma = \sqrt{2}$ , i.e., the motion is on its way to becoming nonrelativistic.

To solve the equations of motion, we therefore proceed as follows. We use the solution given by (32) in the early stages, up to a specified  $\eta_0$ . Starting with  $R = R_1$ ,  $T = T_Q$ , we calculate  $R = R(\eta_0)$  at  $T = T_Q + \eta_0$  by the numerical integration of (32). From this stage onward, we can numerically integrate the full equations (28)–(30) with the starting values provided by the solution of (32).

The numerical details will be discussed in § V. Here we discuss the general features of the solutions. The quasar is fired with a near light speed, but it slows down to nonrelativistic speeds for times of the order of  $\eta_0$ . Subsequently, depending on the value of  $\eta_0$ , it comes to rest at a coordinate value  $R_{\max}(\eta_0)$ . Thereafter it falls back and goes toward  $R = 0$ . If we consider this radial motion as an approximation to a highly eccentric orbit, as in Figure 4, we can carry the integration further by noting the value of  $x$  at  $R = R_1$  and starting again from  $R_1$  with a reversal in the sign of  $x$ . This is tantamount to continuing the orbit “on the other side” of the galaxy. The quasar again comes to rest at a value of  $R$  less than  $R_{\max}(\eta_0)$ , and begins to fall back toward the galaxy.

This radial oscillation (or motion in highly eccentric orbits) continues with decreasing amplitude (decreasing semimajor axis in the case of the orbital motion). The successive orbits are different because the mass of the quasar steadily increases.



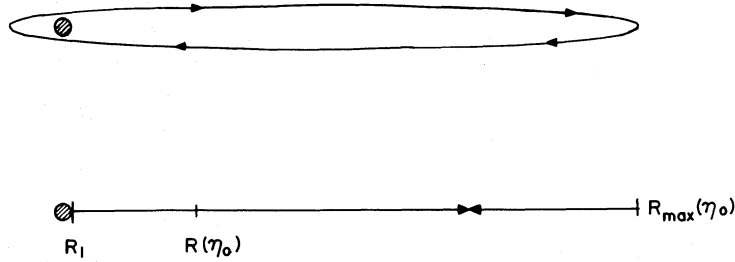


FIG. 4.—A highly eccentric orbit is approximated by a linear motion. Between  $R_1$  and  $R(\eta_0)$  the motion is relativistic in the initial stages.  $R_{\max}(\eta_0)$  denotes the maximum amplitude of the first oscillation.

#### d) The Weak-Field Approximation

The equations (28)–(30) can be reduced to “Newtonian” form for  $M \ll R$ ,  $R \ll T$ ,  $\dot{R} \ll 1$ , and for  $T \gg \eta_0$ . The radial motion is given by

$$\frac{d}{dt}(m\dot{R}) = -\frac{GmM}{R^2}, \quad (36)$$

where  $m$  is a slowly varying function of  $T$ . That is, the change in  $m$  during one oscillation is negligible, compared to the dynamical changes of  $R$ ,  $\dot{R}$ , etc. If we define  $\tilde{t}$  and  $\tilde{G}$  by

$$m\tilde{d}t = m_0 dt, \quad \tilde{G} = G \frac{m^2}{m_0^2}, \quad m_0 = \text{constant}, \quad (37)$$

then (36) becomes

$$\frac{d^2 R}{d\tilde{t}^2} = -\frac{\tilde{G}M}{R^2}. \quad (38)$$

This is motion under a variable gravitational constant. Since the effective gravitational constant increases with time, the successive orbits shrink with time.

We can arrive at this conclusion directly from (23). Consider the simplified case of a circular orbit in the Newtonian approximation of (23). The conservation of angular momentum and the equation of radial balance respectively give

$$mR^2\dot{\theta} = h, \quad mR\dot{\theta}^2 = GmM/R^2, \quad (39)$$

in the standard notation. (Note that as  $m$  is assumed to vary slowly, the right-hand side of [23] is taken as zero.) From (39) we get

$$R = \frac{h^2}{GMm^2} \propto m^{-2}, \quad \dot{\theta} = \frac{G^2 M^2}{h^3} m^3 \propto m^3. \quad (40)$$

Thus the orbits shrink as  $m$  increases with time. Also, the periods of the orbits become shorter.

We now consider applications of these ideas to quasar galaxy pairs.

### V. APPLICATION TO QUASAR-GALAXY ASSOCIATIONS

#### a) A Numerical Example

The observational data about a typical quasar-galaxy (Q-G) association are of the following type: (i) redshift of the quasar =  $z_Q$ ; (ii) redshift of the galaxy =  $z_G$ ; (iii) angular radius of the galaxy =  $\theta_G$ ; (iv) angular separation between the quasar and the galaxy =  $\theta_{QG}$ ; and (v) mass of the galaxy =  $M$ . Of these, information is often not available about (v), and sometimes (iii) is not given. We will assume that (i)–(v) are all known and also take it that the separation between  $Q$  and  $G$  is mostly perpendicular to the line of sight. In a random orientation, the median value of the projected length (perpendicular to line of sight) is  $\sim 0.86$  of the true length of separation. Thus the above assumption is not likely to lead to serious errors.

Using the Einstein–de Sitter cosmology and the relations (4) and (12) as well as the approximation  $T \approx t$ , we get

$$T_Q \approx \frac{2}{3}[(1+z_G)^{-1/2} - (1+z_Q)^{-1/2}]^3, \quad (41)$$

$$T \approx \frac{2}{3}(1+z_G)^{-3/2}. \quad (42)$$

Here  $T_Q$  is the epoch when the quasar was born and  $T$  the epoch when the system was observed (on the  $T$ -scale). At the time of observation the linear separation between the quasar and galaxy was

$$R = 2[1 - (1 + z_G)^{-1/2}](1 + z_G)^{-1}\theta_{QG}. \quad (43)$$

Similarly,  $R_1$ , taken as 10% of the radial extent of the galaxy, is

$$R_1 = \frac{1}{3}[1 - (1 + z_G)^{-1/2}](1 + z_G)^{-1}\theta_G. \quad (44)$$

To explain such a configuration, we have to look for a suitable  $\eta_0$  such that, for the quasar fired at  $T = T_Q$  from  $R = R_1$ , it is at  $R$  given by (43) at  $T$  given by (42).

For example, as reported by Arp (1977), for the quasar-galaxy pair 3C 232 and NGC 3067 we have

$$z_Q = 0.534, \quad z_G = 0.005, \quad \theta_G = 52'', \quad \theta_{QG} = 114'', \quad \text{and} \quad M = 2.7 \times 10^{10} M_\odot. \quad (45)$$

The value of  $M$  is given by Danziger and Chromey (1972). The corresponding values in our dynamical problem are

$$T_Q = 4.58 \times 10^{-3}, \quad T = 0.6617, \\ R = 2.75 \times 10^{-6}, \quad R_1 = 1.26 \times 10^{-7}, \quad M = 2.22 \times 10^{-13}. \quad (46)$$

Numerical computations show that, for  $\eta_0 \sim 10^{-6}$ , it is possible to have orbits which meet these boundary conditions. Therefore although the quasar is initially fired from the galaxy with relativistic speed, provided  $\eta_0$  is of this order, it slows down rapidly to be confined to the neighborhood of the galaxy. This behavior is contrary to the naive expectation based on Newtonian gravity that if a projectile is fired from the galaxy with speed exceeding the "escape speed" of the galaxy, it will never return to the confines of the galaxy.

The value of  $\eta_0$  in the above problem is not unique. Provided they do not exceed a critical value  $\eta_c$  (to be discussed later), we can find more than one  $\eta_0$  to meet the above boundary conditions. This is because for  $\eta_0 < \eta_c$  the quasar describes bound orbits near the galaxy.

The validity of the weak-field approximation discussed in § IVd is borne out by the numerical integrations. A typical example is shown in Figure 5. Note that in the early stages, when the motion is relativistic and  $\ln m$  changes rapidly, this approximation does not hold.

#### b) Bound Quasars

For given  $M$ ,  $R_1$ , and  $T_Q$ , the amplitude of the first oscillation,  $R_{\max}$ , depends on  $\eta_0$ . As we increase  $\eta_0$ ,  $R_{\max}$  increases and so does the time  $T_{\max}$  at which the quasar first turns around. This raises an interesting question. What is the maximum value of  $\eta_0$  for which the turnaround epoch  $T_{\max}$  coincides with the epoch of observation,  $T$ , as given by (42)? We denote this maximum value by  $\eta_c$ . For  $\eta_0 < \eta_c$ , the quasar has definitely turned around at the time of observation and can therefore be regarded as trapped or bound by the galaxy. For  $\eta_0 > \eta_c$  the quasar is still moving

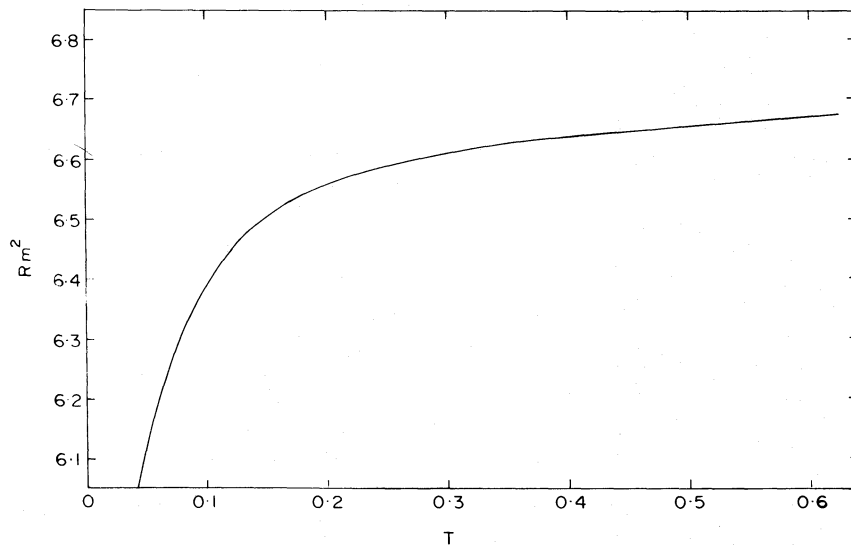


FIG. 5.— $Rm^2$  on an arbitrary scale plotted against  $T$ . The value of  $R$  is taken at the maximum separation from the parent galaxy. We see that  $Rm^2$  approaches a constant value as required in the weak field approximation.

TABLE 1  
CALCULATED MAXIMUM SEPARATION OF BOUND QUASARS FROM THEIR  
PARENT GALAXIES  
(redshift of parent galaxy  $z_G = 0.005$ )

Quasar Redshift $z_Q$	$\eta_c$	$R_{\max}$ (kpc)
Mass of Galaxy $M = 2.7 \times 10^{10} M_\odot$		
0.10 .....	$8.45 \times 10^{-8}$	312
0.50 .....	$1.76 \times 10^{-6}$	292
1.00 .....	$3.85 \times 10^{-6}$	275
2.00 .....	$6.70 \times 10^{-6}$	258
Mass of Galaxy $M = 10^{11} M_\odot$		
0.50 .....	$2.68 \times 10^{-6}$	449
1.00 .....	$5.92 \times 10^{-6}$	428
1.50 .....	$8.40 \times 10^{-6}$	408
2.00 .....	$1.03 \times 10^{-5}$	398

NOTE.— $R_{\max}$  is comparable to but less than  $R_c$ , as given by (21). This bears out the expectation that the influence of the parent galaxy would persist up to distances of the order of  $R_c$ . It is also interesting (and not unexpected) that for the two galaxy masses in the above table,  $R_{\max}$  varies as  $M^{1/3}$ , for the same  $z_Q$ .

away from the galaxy. Although it may turn back at a later epoch, it may be then be considered as having moved too far out to be influenced by the galaxy. Such quasars may be considered free quasars.

We suggest that the bound quasars are those which show up as members of anomalous-redshift quasar-galaxy type combinations, whereas free quasars are those which show no apparent association with a galaxy. Thus we are advocating the hypothesis that *all* quasars were born in galactic explosions but only those with  $\eta_0 < \eta_c$  show up as still associated with their parent galaxies.

In Table 1 we show how  $\eta_c$  is related to the various parameters of the problem.

In typical quasar-galaxy associations, the above values of  $R_{\max}$  should appear as upper bounds. It is worth emphasizing that  $R_{\max}$  is more or less independent of  $z_G$ . For example, for  $z_G = 0.20$ , the value of  $R_{\max}$  for  $z_Q = 1.00$ ,  $M = 2.7 \times 10^{10} M_\odot$  is 240 kpc, as against the value of 275 kpc for  $z_G = 0.005$  in Table 1.

It is now possible to understand the plot of  $\theta_{QG}$  against  $z_G$ , discussed by Burbidge (1979). The near constancy of  $R_{\max}$  with  $z_G$  shows up in the following way. For all bound quasars,  $R_{\max}$  represents the maximum separation from the parent galaxy. In a typical quasar-galaxy pair the separation will in general be less for the following reasons. First, the projection perpendicular to the line of sight is necessarily less than the actual separation, although, as mentioned earlier, in a random orientation this effect will not lead to substantial reduction. A second effect leading to further reduction arises from the fact that a quasar orbiting in a highly eccentric trajectory may not be always seen at maximum separation (apogalacticon). In an average situation the separation may be much less. Time averaging of typical orbits suggests that the two effects together may lead to a median separation which is 10% of the maximum separation. Since  $R_{\max}$  slowly decreases with increasing  $z_G$ , the slightly steeper slope (compared to  $-1$ ) of the best fit line to the  $\log \theta_{QG} - \log z_G$  observed in the data reported by Burbidge (1979) is also to be expected on the basis of this theory.

In Figure 6 the data on  $\theta_{QG}$  from the catalog of Burbidge and Hewitt (1979) is used to plot the median value of  $\theta_{QG}$  against  $z_Q$ . The error bars shown around the median values are indicative of the scatter in the data. The line drawn through the error bars is obtained from Table 1 for  $M = 10^{11} M_\odot$ , with the separation values scaled down to take account of the reduction effects discussed above.

Again, Figure 6 confirms, what is expected on the basis of the above theory, that the separation between quasars and galaxies decreases slowly as  $z_Q$  increases.

### c) Alignments and Redshift Bunching

The observations discussed in § I can be explained within the present framework as follows. First it is not necessary that only one explosion should occur in the lifetime of a galaxy, resulting in the birth of a quasar. Nor is it necessary that only one quasar is created in a single explosion.

If multiple quasar creation takes place in a single explosion, we expect such quasars to have the same redshift, corresponding to the creation epoch  $\tau_Q$ . Thus it is more likely than not to find quasars of the same (or nearly the

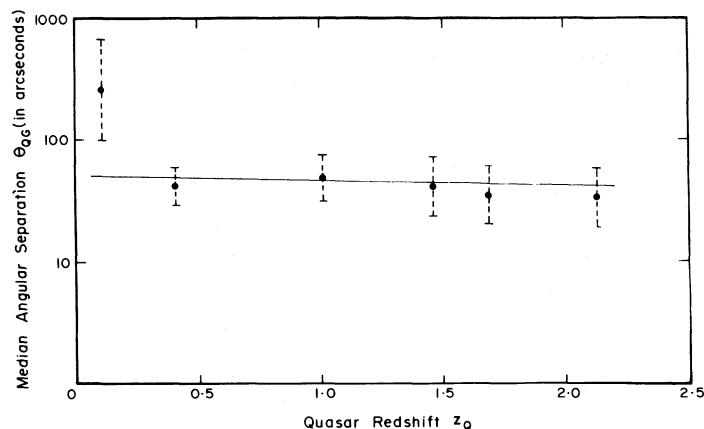


FIG. 6.—The median angular separation plotted against the quasar redshift shows a slow decline as expected from the theory. The high values at low quasar redshifts shown in the first observational point may be due to selection effects. The error-bars are at  $1\sigma$  level.

same) redshifts in the neighborhood of a galaxy. Also, if momentum is conserved in the ejection process, we should see alignments, especially when two quasars are seen near a galaxy. Since the ejection may be with different values  $\eta_0$  for the two quasars, it is not necessary that they are found equidistant from the galaxy, although they may be roughly collinear with the galaxy.

Multiple ejections at different epochs will result in quasars with redshifts bunched around the values corresponding to these epochs. In this connection, it is interesting to review the two triplets mentioned in § I (Arp and Hazard 1979). If we assume, in the present framework, that these triplets are associated with a galactic explosion, then we may try to locate the seat of explosion by joining the pairs of quasars with similar redshifts. As shown in Figure 7, the lines  $AY$ ,  $BX$ , and  $CZ$  pass close to one another in the region close to  $Z$ . It may be worthwhile making a search of this region for a galaxy,  $G$ , or for the remnant of a galaxy which may have been blown apart through three explosions. The observed alignments  $XYZ$  and  $ABC$  arise from projection effects due to our location in the planes of  $X$ ,  $Y$ ,  $Z$  and  $A$ ,  $B$ ,  $C$ .

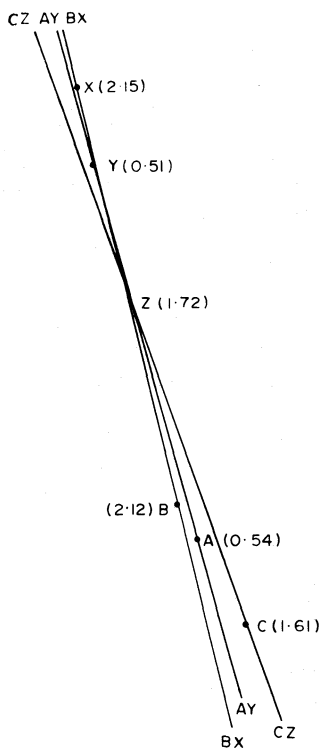


FIG. 7.—The configuration of the two triplets discovered by Arp and Hazard (1979)

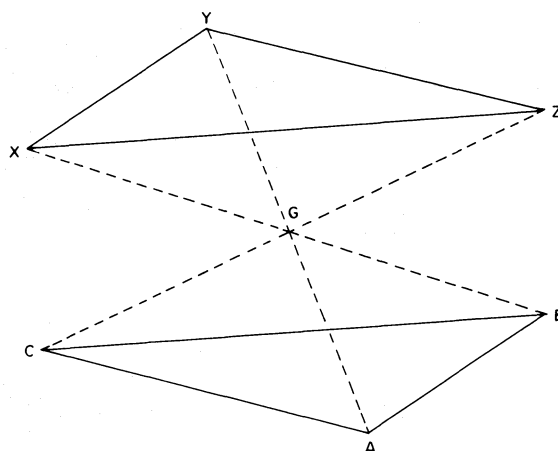


FIG. 8.—An idealized situation to which the two triplets of Fig. 7 may be an approximation. ( $A, B, C$ ) and ( $X, Y, Z$ ) are in parallel planes which, when seen edge-on, give the impression that the three points in each case are collinear.

It is not difficult to see that in a perfectly symmetrical situation, if the quasar pairs are thrown with equal values of  $\eta_0$ , we would have  $GX = GB$ ,  $GY = GA$ , and  $GZ = GC$ ; and the planes  $XYZ$  and  $ABC$  would be parallel, as shown in Figure 8. Our location in these planes would then produce apparently linear systems  $XYZ$  and  $ABC$ . The situation in Figure 7 may be considered a slight distortion of the highly symmetrical situation of Figure 8.

In general we suggest that if the anomalous redshift observations are to be taken seriously, then according to the present theory alignments and redshift bunching should be expected and looked for.

#### VI. OTHER TESTS OF THE LOCAL HYPOTHESIS

Alignments and redshift bunching are effects expected in the theoretical framework described here. As discussed in § II, it is difficult to see how these effects could be explained in the other, more conventional, interpretations of redshifts. Therefore if future observations on quasar-galaxy associations do show these effects, then this should constitute a strong point in favor of the theory described here.

Apart from these effects, there are other possible tests which may be used in future to test the validity of this theory. Briefly they are as follows.

1. The age of an object is usually measured from the zero mass epoch on its world line. Hence the higher the redshift of the quasar, the younger it is. Although except in the context of stars, where nuclear reactions and abundances provide some age criteria, there is no reliable age indicator for astronomical objects, in this theory we can use any information that is obtainable from the age dependence of the masses of elementary particles in the quasar. For example, if a quasar of redshift 2 is seen in association with a galaxy of very low redshift, say  $z_G \sim 0.005$ , then the electron mass in the latter is 3 times the electron mass in the former. This effect must be included in any criterion used for estimating the age of the quasar, such as its morphology, nuclear abundance, etc.

2. The redshift dependence of particle masses in a quasar should show up in its luminosity. For example, if a synchrotron mechanism is responsible for emission from the quasar, then we expect the rest frame luminosity in the quasar to be higher by the factor  $(1 + z_0)^2$ . This estimate is based on the assumption that the ambient magnetic field is not dependent on the state of the matter in the quasar but is provided by the galaxy. The lifetime of the electrons, the spectrum of radiation, etc., need to be carefully examined before testable predictions can be made.

3. If the associations found by Stockton (1978) as well as by Arp are real, then we have quasars ranging over distances from  $\sim 30$  Mpc to  $\sim 2000$  Mpc. This corresponds to a variation in the apparent magnitude of  $\sim 9$  mag for quasars of the same absolute magnitude. Or, two quasars of the same apparent magnitude but located over distances of 30 Mpc and 2000 Mpc must vary in intrinsic luminosity by a factor  $\sim 5000$ . While this makes the quasar population more inhomogeneous than if all quasars were at cosmological distances, or if all quasars were at  $\sim 30$ – $100$  Mpc, the luminosity spread in itself cannot be taken as a disproof of this hypothesis. After all, stars as a whole show a much wider spread in luminosity. Whether there exist quasars of two populations may be decidable with the help of the number-magnitude counts of quasars. By going to faint enough magnitudes the “local” component may drop and the distant component pick up, thus leading to a discontinuity in the slope of the curve. It would be worth looking for this effect as the techniques of quasar number counts improve. Counts of X-ray quasars may also help in deciding the issue.

4. Any effects leading to the information about the column density of the intervening medium from the Galaxy to the quasar can also help in deciding whether quasars are local. Effects like absorption on the blue side of Lyman- $\alpha$  should therefore be looked for.



So far as this theory is concerned, in calculating any such effects and relating them to observations, it must be remembered that the quasar matter is made up of particles of *lower* mass than found in ordinary matter. The basic framework of this theory enables one to make such calculations unambiguously. We propose to discuss some of these effects in a future paper.

One of us (J. V. N.) would like to thank Drs. Geoffrey Burbidge and Chip Arp for critical comments and discussions. We also thank Drs. Burbidge and A. Hewitt for the use of their catalog of quasi-stellar objects and are grateful to Mr. H. M. Antia and Mr. S. N. Pandey for help in numerical computations.

## REFERENCES

- Arp, H. 1977, *IAU/CNRS Colloquium* (Paris: CNRS), p. 377.  
 ———. 1980a, *Ap. J.*, **236**, 63.  
 ———. 1980b, preprint.  
 Arp, H., and Hazard, C. 1979, preprint.  
 Arp, H., Sulentic, J. W., and di Tullio, G. 1979, *Ap. J.*, **229**, 489.  
 Bondi, H. 1964, *Proc. Roy. Soc. A*, **282**, 303.  
 Burbidge, G. R. 1979, *Nature*, **282**, 451.  
 Burbidge, G. R., and Burbidge, E. M. 1967, *Quasi-Stellar Objects* (San Francisco: Freeman).  
 Burbidge, G. R., and Hewitt, A. H. 1979, preprint.  
 Danziger, I. J., and Chromey, F. R. 1972, *Ap. Letters*, **10**, 99L.  
 Das, P. K. 1976, *M.N.R.A.S.*, **177**, 391.  
 Das, P. K., and Narlikar, J. V. 1975, *M.N.R.A.S.*, **171**, 87.  
 Hoyle, F. 1975, *Ap. J.*, **196**, 661.  
 Hoyle, F., and Burbidge, G. R. 1966, *Ap. J.*, **144**, 534.  
 Hoyle, F., and Fowler, W. A. 1967, *Nature*, **213**, 373.  
 Hoyle, F., and Narlikar, J. V. 1964, *Proc. Roy. Soc. A*, **282**, 191.  
 ———. 1974, *Action at a Distance in Physics and Cosmology* (San Francisco: Freeman).  
 Kembhavi, A. K. 1978, *M.N.R.A.S.*, **185**, 807.  
 Narlikar, J. V. 1977, *Ann. Phys.*, **107**, 325.  
 Stockton, A. 1978, *Ap. J.*, **223**, 747.  
 Terrell, J. 1964, *Science (N.Y.)*, **145**, 918.

P. K. DAS: Indian Institute of Astrophysics, Sarjapur Road, Bangalore 560 034, India

J. V. NARLIKAR: Tata Institute of Fundamental Research, Homi Bhabha Road, Bombay 400 005, India